Journal of Organometallic Chemistry 738 (2013) 41–48

Contents lists available at SciVerse ScienceDirect

Journal of Organometallic Chemistry

journal homepage: www.elsevier.com/locate/jorganchem

Facile synthesis of 5-substituted-1*H*-tetrazoles and 1-substituted-1*H*-tetrazoles catalyzed by recyclable 4′-phenyl-2,2′:6′,2″-terpyridine copper(II) complex immobilized onto activated multi-walled carbon nanotubes

Hashem Sharghi*, Sakineh Ebrahimpourmoghaddam, Mohammad Mahdi Doroodmand

Department of Chemistry, College of Sciences, Shiraz University, Shiraz 71454, Iran

ARTICLE INFO

Article history:
Received 9 December 2012
Received in revised form
5 April 2013
Accepted 10 April 2013

Keywords:
Carbon nanotube
Heterogeneous
Recyclable
Terpyridine copper complex
Tetrazole

ABSTRACT

5-Substituted-1*H*-tetrazoles can conveniently be synthesized from the corresponding nitriles by reaction with NaN_3 using the efficient and recyclable heterogeneous catalyst prepared by immobilization of copper(II) complex of 4′-phenyl-2,2′:6′,2″-terpyridine on activated multi-walled carbon nanotubes [AMWCNTs-O–Cu(II)–PhTPY]. Excellent results were obtained in each case affording the corresponding tetrazole adducts in good to excellent yields. In general, aromatic nitriles with electron-donating group could be accomplished as well as that with electron-withdrawing groups. By leaving out nitrile from the reaction and adding $CH(OEt)_3$ and amines bearing various substituents, 1-substituted-1*H*-tetrazoles formed in water in high yields. The reported protocols have the advantages of rapid assembly of a host of heterocyclic systems in high yields with the added advantage of recycling and reuse of the catalyst.

1. Introduction

The chemistry of heterocycles has acquired immense importance in recent years. Tetrazoles which represent an important class of heterocycles are an increasingly popular functionality with wide ranging applications [1]. In particular, this functional group have shown strong activities as sedatives [2], antihypertensive drugs [2], antiallergic [2], antimicrobial [3], antibacterial [4], antifungal [5], carboxylic acid isosteres [6], anti-imflammatory [7], hormonal [8], diuretics activity [9], and herbicides [10]. These nitrogen-rich ring systems have also applications in material science including propellants [11], explosives [12] and photography [13]. Furthermore, tetrazole moieties are important synthons in synthetic organic chemistry [14]. They form stable complexes with metals [15] and have been used as ligands for palladium-catalyzed reactions [16].

Because of their potent usefulness, the synthesis of tetrazole frameworks has received much attention recently, and various preparative methods have been developed. For tetrazole ring construction the synthetic equivalents of sodium azide or organic azides and cyanides, isocyanides, isocyanates or isothiocyanates are used most frequently [17]. They can be brought into the reaction as individual compounds or generated directly in a reaction medium [14]. Another method of a tetrazole ring synthesis is based on the reaction of amines with triethyl orthoformate and sodium azide [18,19]. Whereas the [3 + 2] cycloaddition of isocyanides with $TMSN_3$ under the influence of various catalysts reported by Yamamoto et al. [20] provides access to various 1-substituted tetrazoles, reaction of primary amines with orthocarboxylic acid ester/sodium azide reported in several more recent reports is more practical. The use of $In(OTf)_3$ and $Yb(OTf)_3$ as catalysts for this three component transformation has been reported utilizing alcoholic solvents or neat at high temperatures (100 °C) [18,21]. Catalysis by 1-*n*-butylimidazolium tetrafluoroborate with $NaN_3/CH(OEt)_3$ has also been shown, but it requires high temperatures [22]. Some of these methods have one or more of the following drawbacks: expensive and toxic metal catalysts, harsh reaction conditions, refluxing for a prolonged period of time and tedious work-ups. All of these approaches reveal that the catalytic formation of these classes of heterocyclic compounds is still challenging and that the area demands to be developed further.

Heterogeneous-reagent systems have many advantages such as simple experimental procedures, mild reaction conditions and the minimization of chemical wastes as compared to their liquid phase counterparts [23]. Catalysis is currently recognized as a potential field of application for carbon nanotubes (CNTs), and throughout the past decade the number of publications and patents on this subject has been increasing exponentially [23].

* Corresponding author. Fax: +98 711 2280926.
E-mail addresses: hashemsharghi@gmail.com, shashem@chem.susc.ac.ir (H. Sharghi).

0022-328X/$ – see front matter © 2013 Elsevier B.V. All rights reserved.
http://dx.doi.org/10.1016/j.jorganchem.2013.04.013

In continuation of our work on synthesis of biologically active heterocyclic scaffolds [23], we report here on the use of immobilized 4′-phenyl-2,2′:6′,2″-terpyridine copper(II) complex onto activated multi-walled carbon nanotubes for facile construction of 5-substituted-1*H*-tetrazoles, and 1-substituted-1*H*-tetrazole ring systems in high yields under very mild conditions with recycling and reuse of the heterogeneous catalyst (Scheme 1).

2. Experimental section

2.1. Instrumentation, analysis, materials and general experimental details

NMR spectra were recorded on a Bruker Avance DPX-250 (^{1}H NMR 250 MHz and ^{13}C NMR 62.9 MHz) in pure deuterated solvents with tetramethylsilane (TMS) as internal standards. Scanning electron micrographs were obtained by SEM instrumentation (SEM, XL-30 FEG SEM, Philips, at 20 kV). An atomic forced microscopy (AFM, DME-SPM, version 2.0.0.9) was also used for AFM images. FT-IR spectroscopy (Shimadzu FT-IR 8300 spectrophotometer) were employed for characterization of the heterogeneous catalyst. The TG analysis of the samples was carried out using a labmade TG analyzer instrument. Metal contents were obtained by an ICP analyzer (Varian, vista-pro). Mass spectra were determined on a Shimadzu GCMS-QP 1000 EX instrument at 70 or 20 eV. Melting points determined in open capillary tubes in a Buchi-535 circulating oil melting point apparatus. UV/Vis spectra was obtained with an Ultrospec 3000 UV/Visible spectrometer. Elemental analyses were performed on a Thermo Finnigan CHNS-O analyzer, 1112 series. The purity determination of the substrates and reaction monitoring were accomplished by TLC on silica gel PolyGram SILG/UV254 plates or by a Shimadzu Gas Chromatograph (GC-10 A) instrument with a flame-ionization detector using a column of 15% carbowax 20 M chromosorb-w acid washed 60–80 mesh. Column chromatography was carried out on short columns of silica gel 60 (70–230 mesh) in glass columns (2–3 cm diameter) using 15–30 g of silica gel per 1 g of crude mixture. Chemical materials were either prepared in our laboratories or were purchased from Fluka, Aldrich and Merck Companies.

2.2. Synthesis of catalyst

2.2.1. Preparation of 4′-phenyl-2,2′:6′,2″-terpyridine

The ligand 4′-phenyl-2,2′:6′,2″-terpyridine was synthesized according to the literature method and characterized by NMR, IR, Mass and elemental analysis [23]. Pale yellow crystals; 0.15 g, 47% yield. M.p. = 122–125 °C. IR (KBr): 682(m), 893(m), 1041(m), 1267(m), 1465(s), 1583(s) cm^{-1}. ^{1}H NMR ($CDCl_3$, 250 MHz): δ = 7.07–7.42(m, 5H), 7.71–7.81(m, 4H), 8.53–8.67(d, J = 7.5 Hz, 2H), 8.59–8.62(d, J = 7.5 Hz, 2H), 8.63(s, 2H) ppm. ^{13}C NMR ($CDCl_3$, 62.9 MHz): δ = 118, 121, 123, 127, 128, 129, 136, 138, 149, 150, 155, 156 ppm. MS: m/z (%) = 310(66.5) $[M + 1]^+$, 309(98.8) $[M]^+$, 231(61.3), 209(41.0), 176(12.1), 106(38.7), 78(97.1). C_{21} H_{15} N_3 (309.360): C 81.53, H 4.89; found C 81.37, H 4.74.

2.2.2. Preparation of 4′-phenyl-2,2′:6′,2″-terpyridine copper (II) complex

The compound 4′-phenyl-2,2′:6′,2″-terpyridine (6.18 mg, 0.02 mmol) was added to solution of $Cu(CH_3COO)_2.H_2O$ (4 mg, 0.02 mmol) in water (2 mL). Stirring for 0.5 h at room temperature resulted in a clear blue–green solution. This solution was used as homogeneous catalyst.

2.2.3. Synthesis of multi-walled carbon nanotubes

MWCNTs were synthesized by the chemical vapor deposition (CVD) process using acetylene as the source of carbon and ferrocene as the source of iron nanoparticles at temperature to ~1300 °C in an inert atmosphere of argon. Trace flow of oxygen in argon was introduced to the CVD production line for purification of MWCNTs from any amorphous carbon or bulky nanomaterials such as fullerene, opening the CNT bundles, and activation of the carbon nanostructures to form hydroxyl functional groups. To synthesize MWCNTs, briefly, 5% molar percentage of ferrocene solution in benzene was used for production of Fe nanoparticles (diameter 2–10 nm), followed by decomposition of acetylene, generation of carbon vapors and finally deposition onto the metal nanoparticles. The synthesized MWCNT bundles were then directly purified by purging with oxygen and nitric acid vapors. In accordance with the TG analysis and Raman spectroscopy, the purity of the MWCNT bundles was estimated to ~99%.

2.2.4. Activation of multi-walled carbon nanotubes

In order to develop hydroxyl groups on the surface for better anchoring the metal complex, high temperature air activation method was utilized. A tubing resistance furnace with 150 mm diameter and ~1.0 m length, with the two ports open, was initially set to 700 °C. The purification step was achieved in an on-line process, followed by the synthesis of MWCNTs by CVD method. The quartz tube carrying the MWCNTs by the flow of argon was placed in the center of the furnace tube. Temperature was maintained at 700 °C, while the argon was flown with ~200 mL min^{-1} flow rate. So that MWCNTs were mixed with air to produce the desired AMWCNTs.

2.2.5. Preparation of AMWCNTs-ONa

Suspension of AMWCNTs with hydroxyl functional group (1 g) in an alkaline solution of NaOH (10 N, 30 mL) was refluxed for 2 h. The resulting black precipitate was filtered through a celite pad, washed with water until PH received 8–9. The black solid was dried in vacuo to afford the MWCNTs-ONa (1 g).

2.2.6. Immobilization of 4′-phenyl-2,2′:6′,2″-terpyridine copper(II) complex onto AMWCNTs

AMWCNTs-ONa (0.5 g) was added to a freshly prepared aqueous [Cu(II)–PhTPY] (0.5 mmol, 20 mL) solution, the mixture was sonicated

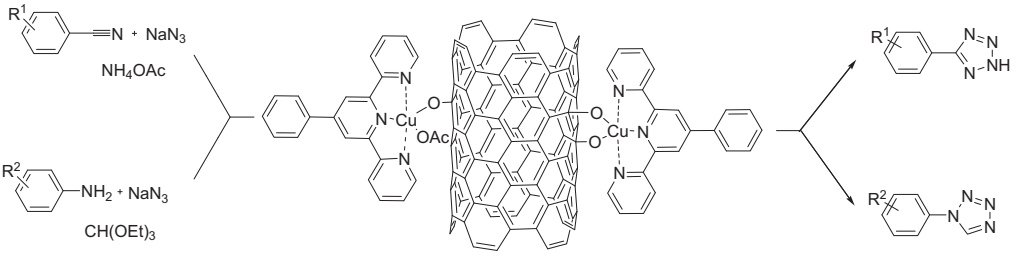

Scheme 1.

for 1 h and stirred at room temperature for 24 h. The resulting black precipitate was filtered through a celite pad, washed with water (25 mL), MeOH (25 mL), and ether (25 mL), dried in vacuum to afford the [AMWCNTs-O–Cu(II)–PhTPY] as a black solid.

2.3. General procedure for the synthesis of 5-substituted-1H-tetrazoles derivatives in the presence of a catalytic amount of the [AMWCNTs-O–Cu(II)–PhTPY] and recycling of the heterogeneous catalyst

The [AMWCNTs-O–Cu(II)–PhTPY] heterogeneous catalyst was subjected to 5 successive reuses under the reaction conditions: For each reaction, nitrile (1.0 mmol), NaN_3 (1.3 mmol) and NH_4OAc (1.0 mmol) were mixed and stirred in DMF (1 mL) in the presence of 4 mol-% of [AMWCNTs-O–Cu(II)–PhTPY] at 70 °C in an uncapped vial. After the completion of the reaction, as monitored by TLC using *n*-hexane/ethyl acetate, the mixture was diluted by H_2O (5 mL), then the mixture was vacuum-filtered onto a sintered-glass funnel, and the residue was consecutively washed with ethyl acetate (30 mL), water (5 mL). The heterogeneous catalyst was recharged for another reaction run. The combined supernatant and organic washings were extracted with ethyl acetate (3 × 10 mL), the combined organic layer was dried over anhydrous Na_2SO_4. Removal of the solvent under vacuum, followed by purification on silica gel using hexane/ethyl acetate as the eluent afforded the pure products.

2.4. General procedure for the synthesis of 1-substituted-1H-tetrazoles derivatives in the presence of a catalytic amount of the [AMWCNTs-O–Cu(II)–PhTPY]

Amine (1.0 mmol), $HC(OEt)_3$ (1.0 mmol) and NaN_3 (1.3 mmol) were mixed and stirred in water (2 mL) in the presence of 4 mol-% of [AMWCNTs-O–Cu(II)–PhTPY] at 70 °C in an uncapped vial. After the completion of the reaction, as monitored by TLC using *n*-hexane/ethyl acetate, the mixture was diluted by H_2O (5 mL), then the mixture was vacuum-filtered onto a sintered-glass funnel, and the residue was consecutively washed with ethyl acetate (30 mL), water (5 mL). The combined supernatant and organic washings were extracted with ethyl acetate (3 × 10 mL), the combined organic layer was dried over anhydrous Na_2SO_4. Removal of the solvent under vacuum, followed by purification on silica gel using hexane/ethyl acetate as the eluent afforded the pure products.

3. Results and discussion

In chemical and pharmaceutical industries, recycling of homogeneous catalysts has great economic and environmental importance.

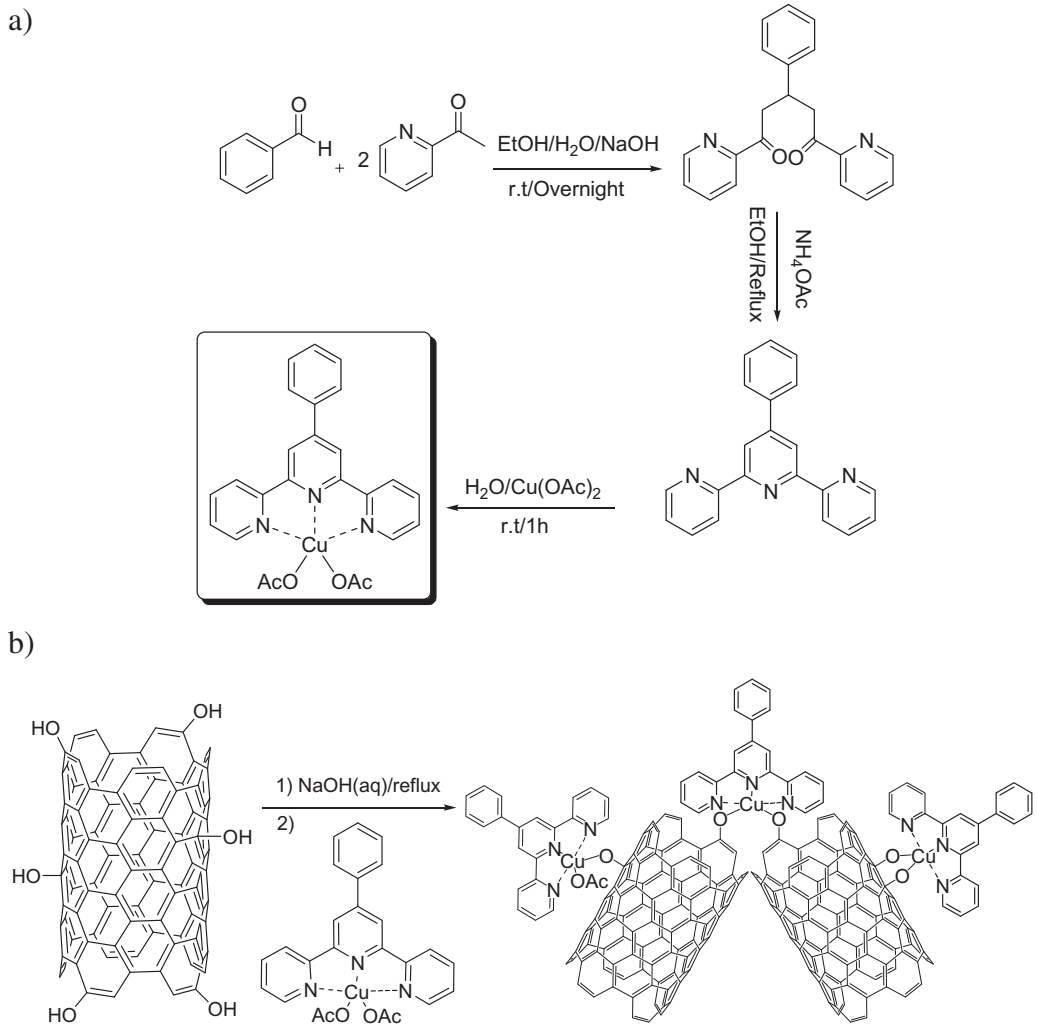

Scheme 2. a) Synthesis of 4′-phenyl-2,2′:6′,2″-terpyridine copper(II) complex, b) Immobilized 4′-phenyl-2,2′:6′,2″-terpyridine copper(II) complex onto activated multi-walled carbon nanotubes [AMWCNTs-O–Cu(II)–PhTPY].

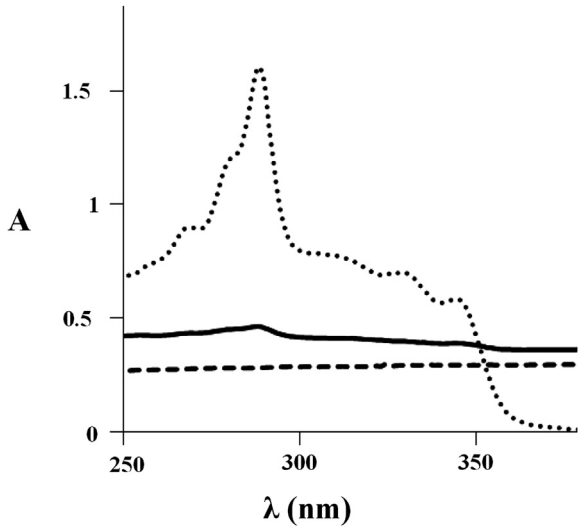

Fig. 1. UV/Vis. spectra of AMWCNTs (——), [AMWCNTs-O–Cu(II)–PhTPY] (▪) and [Cu(II)–PhTPY] (….), obtained in ethanol.

Homogeneous catalysts immobilization on various insoluble solid supports with high surface areas is usually the method of choice, since the immobilized catalysts can be facilely recovered via a simple filtration process after reactions [24]. Catalysis is currently recognized as a potential field of application for carbon nanotubes (CNTs), and throughout the past decade, the number of publications and patents on this subject has been increasing exponentially [25]. In the most cases, the use of these nanomaterials as solid supports have better performances than conventional supports. Indeed, CNTs represent an interesting alternative to conventional support structures because of their high purity that eliminates self-poisoning, high electrical conductivity and thermal stability, impressive mechanical properties, high accessibility of the active phase, absence of any microporosity, eliminating diffusion and intraparticle mass transfer in the reactions medium, the possibility for macroscopic shaping of the support, the possibility of tuning the specific metal–support interactions, which can directly affect the catalytic activity and selectivity; and finally the possibility of confinement effects in their inner cavity. Additionally, compared to conventional supports, CNTs have a high flexibility for the dispersion of the active phase, since it is possible to modulate their specific surface area (50–500 $m^2\ g^{-1}$ for multi-walled carbon nanotubes (MWCNTs)) or their internal diameter (5–100 nm for MWCNTs), ease of chemical functionalization of their surfaces, change their chemical composition (nitrogen- or boron-doped CNTs), and deposit lots of catalytic phase either on their external surface or in their inner cavity [26].

3.1. Characterization of heterogeneous catalyst

We have recently reported the use of activated multi-walled carbon nanotubes as a feasible support for 4′-Phenyl-2,2′:6′,2″-terpyridine copper(II) complex [AMWCNTs-O–Cu(II)–PhTPY] [23], which has been applied as the catalyst for Huisgen's [3 + 2] azide-alkyne cycloaddition, a three-component *click reaction* in water. Now in this report, we have presented another highly useful catalytic application of this catalyst for synthesis of tetrazole systems.

The catalyst was prepared and characterized according to our previously reported protocol (Scheme 2) [23]. 4′-Phenyl-2,2′:6′,2″-terpyridine was synthesized according to a modified Krönke procedure. The copper complex was obtained by adding 4′-phenyl-2,2′:6′,2″-terpyridine to an aqueous solution of copper(II) acetate monohydrate, and the mixture was stirred for 1 h, resulting in a blue–green solution. Before direct use of the MWCNTs, their surface was activated via introduction hydroxy (OH) groups by means of gas phase oxidation under air. This modification booms the reactivity of CNTs and allows for easier deposition of the metal precursors at the nucleating sites; thus, higher catalyst dispersions are to be expected. Firstly, AMWCNTs-ONa was obtained via refluxing of AMWCNTs in an alkaline solution. Then, it was added in to a freshly prepared aqueous solution of [Cu(II)–PhTPY]. Finally, the mixture was sonicated for 1 h and stirred at room temperature for 24 h. The resulting black precipitate was filtered through a celite pad, washed with water, MeOH and ether, dried in vacuum to afford the [AMWCNTs-O–Cu(II)–PhTPY] as a black solid.

The resulting immobilized copper complex on AMWCNTs were characterized by UV–Vis spectroscopy. In Fig. 1 the absorption spectra of free [Cu(II)–PhTPY], AMWCNTs, and [AMWCNTs-O–Cu(II)–PhTPY] in ethanol are compared. [Cu(II)–PhTPY] absorbs light at 288 nm and 320–350 nm showing sharp bands with fine structures. The spectrum of AMWCNTs does not show any fine structure; however, a continuous absorption is evident. According to Fig. 1, the spectrum of [AMWCNTs-O–Cu(II)–PhTPY] reveals that the characteristic absorption bands of [Cu(II)–PhTPY] in the [AMWCNTs-O–Cu(II)–PhTPY] are evidently broaden as compared with the free [Cu(II)–PhTPY], although the exact comparison at the same [Cu(II)–PhTPY] concentration is impossible due to the masking effect from AMWCNTs [27]. These observations verify efficient complex formation between [Cu(II)–PhTPY] and AMWCNTs. Treatment of [AMWCNTs-O–Cu(II)–PhTPY] with EDTA solution resulted in the disappearance of the characteristic absorptions due to [Cu(II)–PhTPY], indicating that EDTA dissociate the [Cu(II)–PhTPY] by liberating tpy ligand absorbing at 235–290 nm (see Supporting Information, Figure S1).

Transmission electron microscopy (TEM) and scanning electron microscopy (SEM) images of the catalyst show the morphology of catalyst, when doped with copper complex (Fig. 2). In order to obtain more information about the topography of the surface of the

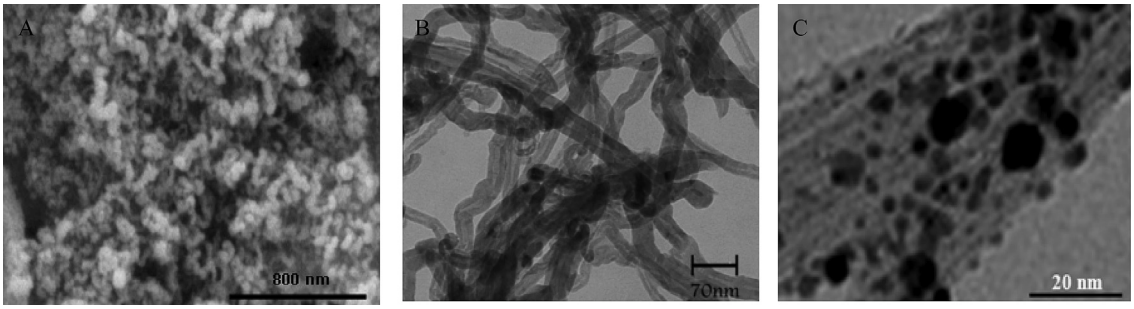

Fig. 2. A) SEM, B) TEM, C) TEM with higher resolution of the immobilized copper complex on AMWCNTs.

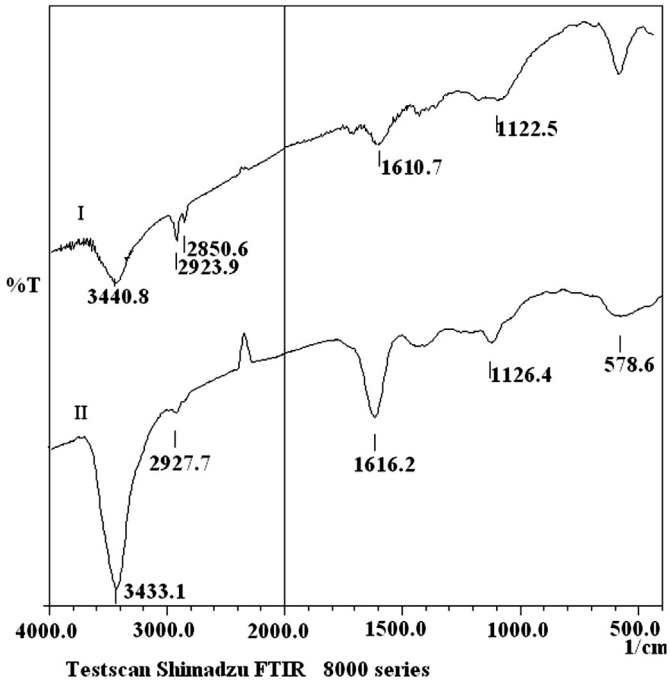

Fig. 3. FT-IR spectra of I) AMWCNTs and II) [AMWCNTs-O–Cu(II)–PhTPY].

prepared catalyst, we have also presented the AFM image of the catalyst (see Supporting Information, Figure S2).

The width of the band at half height of the voltage profile peak reveals the size of copper(II) complexes nanoparticles. From AFM images, the histogram related to the frequency percentages of the average of different sizes of copper complexes on AMWCNTs obtained. According to this histogram, the diameter of copper complexes is ranged from 2.5 to 40 nm (see Supporting Information, Figure S3). The amount of copper complex content supported on AMWCNTs was determined by ICP analysis techniques to be 4.895%. The thermal stability of copper-doped AMWCNTs was also investigated using a TG analysis instrumentation system. The thermogram of the sample at an air flow rate of 2.0 mL min^{-1} and a temperature ramp of 2.0 °C min^{-1}. Based on this thermogram, significant change at ~210 °C is related to the decomposition of ligand. Also, a decrease enhancement at ~400 °C is due to the oxidation of copper and formation of copper oxide (CuO). Whereas, significant decrease in the weight percentage of the thermogram at ~610 °C is related to the decomposition of AMWCNTs (see Supporting Information, Figure S4). In this study, no significant changes were observed in the active surface area of the copper-doped AMWCNTs, compared to AMWCNTs as evaluated via following the nitrogen adsorption capacity of both AMWCNTs and copper-doped AMWCNTs (see Supporting Information, Figure S5).

The process related to the complex formation of the nanocatalyst was also evaluated using FT-IR spectrometry. Fig. 3I and II shows the FT-IR spectra of AMWCNTs and [AMWCNTs-O–Cu(II)–PhTPY], respectively. Based on the FT-IR spectra (Fig. 3II), sharp peak at 578.6 cm^{-1} is related to the formation of Cu–O bond [23]. Whereas, the broad peak positioned around 1616.2 cm^{-1}, is correlated to the C=C bond presented in the CNT matrix overlapped with the copper complexed moieties [28]. It seems that, low amounts of copper complex on the CNTs surface lead to the peak broadening in the [AMWCNTs-O–Cu(II)–PhTPY] system. The amounts of hydroxyl group were also estimated to 6.11% based on the back titration process.

3.2. Synthesis of 5-substituted-1H-tetrazoles

To evaluate the merit of application of this catalytic system in organic synthesis, we applied it in the [3 + 2] cycloaddition of nitriles and azide. Initial studies were performed upon the reaction of 4-methylbenzonitrile with NaN_3 as a model reaction and the effects of different conditions were studied for this reaction (Table 1). In order to create a procedure that avoids the use of high amount of catalyst, ammonium acetate was used as proton source to provide the pure tetrazoles. Thanks to the low p*K*a of 1*H*-tetrazoles (ca. 3–5) and their highly crystalline nature [29], a simple acidification is usually sufficient to break the metal-nitrogen bond.

According to Table 1, when the model reaction was performed under catalyst-free conditions at 100 °C, the desired product was obtained in low yield (Table 1, Entry 1). Although, copper acetate

Table 1
Comparison of the conditions used for the reaction of 4-methylbenzonitrile with NaN_3..

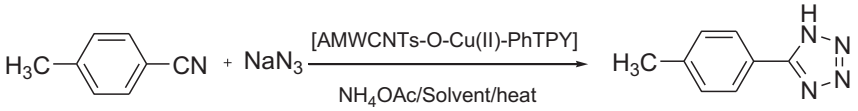

Entry	Solvent	Temperature (°C)	Catalyst (mol%)	Time (h)	Yield (%)[a]
1	DMF	100	–	5	30
2	DMF	100	$(CH_3COO)_2Cu·H_2O$ (2)	5	50
3	DMF	100	[Cu(II)–PhTPY] (2)	5	90
4	DMF	100	[AMWCNTs-O–Cu(II)–PhTPY] (2)	5	100
5	None	100	[AMWCNTs-O–Cu(II)–PhTPY] (2)	5	10
6	DMSO	100	[AMWCNTs-O–Cu(II)–PhTPY] (2)	5	70
7	Dioxane	100	[AMWCNTs-O–Cu(II)–PhTPY] (2)	5	60
8	CH_3CN	Reflux	[AMWCNTs-O–Cu(II)–PhTPY] (2)	5	50
9	DMF	80	[AMWCNTs-O–Cu(II)–PhTPY] (2)	5	80
10	DMF	70	[AMWCNTs-O–Cu(II)–PhTPY] (2)	5	80
11	DMF	50	[AMWCNTs-O–Cu(II)–PhTPY] (2)	5	30
12	DMF	30	[AMWCNTs-O–Cu(II)–PhTPY] (2)	5	5
13	DMF	70	[AMWCNTs-O–Cu(II)–PhTPY] (4)	4	100
14	DMF	70	[AMWCNTs-O–Cu(II)–PhTPY] (6)	4	100
15	DMF	70	[AMWCNTs-O–Cu(II)–PhTPY] (8)	4	100

[a] Determined by ^1H NMR spectroscopy.

could accelerate the reaction to produce the target compound, it could not provide satisfactory yields (Table 1, Entry 2). We observed an increase in the reaction yield using [Cu(II)–PhTPY] (2.0 mol %) at 100 °C (Table 1, Entry 3).

The results showed that among the tested conditions, using [AMWCNTs-O–Cu(II)–PhTPY] as catalyst and DMF as solvent were more efficient in which the desired product was obtained in higher yields than the other solvents under study (Table 1, Entry 4). In the reactions employing DMSO, dioxane and CH_3CN as the solvents, the reactions did not progress efficiently and after 5 h, the desired product was obtained in 50–70% yields (Table 1, Entries 6–8). Lowering the temperature to 80 and 70 °C led to decrease in reaction yields (Table 1, Entry 9 and 10). Reducing the temperature to 50 and 30 °C was accompanied by a considerable drop of yield by 30 and 5%, respectively (Table 1, Entry 11 and 12). We have also investigated the effect of different amount of catalyst upon the reaction. By increasing of the catalyst loading to 4.0 mol % the reaction completed after 4 h at 70 °C. However, using higher amount of catalyst has no significant effect on reaction rate and isolated yield of product (Table 1, Entries 14 and 15).

Study for optimization of the reaction with respect to the amounts of the starting materials and the catalyst, led us to nitrile (1 mmol), azide (1.3 mmol), DMF (1.0 mL), NH_4OAc (1 mmol) and catalyst (4.0 mol%) at 70 °C (Scheme 3). As a result of these endeavors, we have found that in the presence of [AMWCNTs-O–Cu(II)–PhTPY], tetrazole formation proceeds with excellent yields and scope in DMF (Table 2).

As shown in Table 2, a range of nitriles reacted with NaN_3 to give the desired products. Employing the optimized catalytic conditions, nitriles bearing electron-donating groups provided high yields of the desired products (Table 2, Entries 1–3). Similarly, the reactions of substrates with electron-withdrawing group as well as heteroaryl nitriles with azide were also studied (Table 2, Entries 4–14). As shown in Table 2, the reaction of nitriles having a NO_2, CF_3 or CN functional group in *para* position went to completion within 1.0, 0.8 and 1.5 h to give tetrazole in excellent yield (Table 2, Entry 4, 5 and 10). It is noticeable that, compared to electron-rich nitriles, electrondeficients furnished the corresponding products in shorter reaction time and comparatively higher reaction yields. Steric hindrance also shows its effects upon the rates of the reactions. As the example, 4-methylbenzonitrile reacted with azide within 4 h with the isolation of the desired product in 90% (Table 2, Entry 1). Although, the similar reaction with 2-methylbenzonitrile was performed in 7 h producing the final product in 75% yield (Table 2, Entry 2). Similarly, longer reaction time has been observed for the reaction of phthalonitrile with azide (Table 2, Entry 12).

A plausible mechanism is shown in Scheme 4. Initially, [Cu (II) TPY] nano-catalyst reacts with azide to produce the [Cu (II) TPY]–N_3 (**I**) catalytic species. The [3 + 2] cycloaddition between the C–N bond of nitrile and (**I**) takes place to form the intermediate (**II**). Precoordination of the nitrogen atom of the CN group of **2** with (**I**) to form complex (**II**) would accelerate this cyclization step. Protonolysis of the intermediate (**II**) by H^+ of NH_4OAc affords the 5-substituted-1*H*-tetrazole (III) and copper catalyst.

3.3. Activity and reusability of heterogeneous catalyst

The model reaction (4-methylbenzonitrile, NaN_3 in a 1:1.3 M ratio in DMF at 70 °C) was performed successfully within 4 h in the

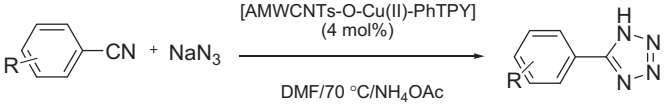

Scheme 3. Synthesis of 5-substituted 1*H*-tetrazol.

Table 2
Synthesis of 5-substituted 1*H*-tetrazoles.

Entry	Nitrile	Product	Time [h]	Yield [%][a]
1	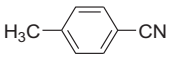	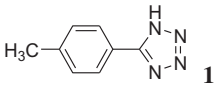 **1**	4.0	90
2	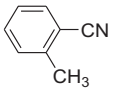	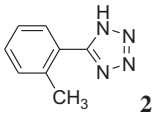 **2**	7.0	75
3	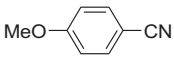	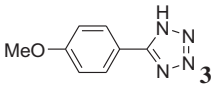 **3**	6.0	90
4	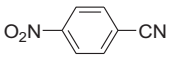	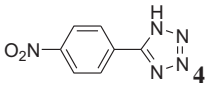 **4**	1.0	92
5	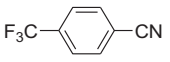	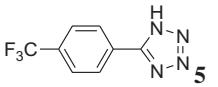 **5**	0.8	98
6	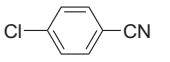	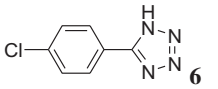 **6**	2.5	90
7	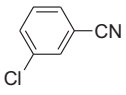	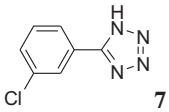 **7**	2.0	85
8	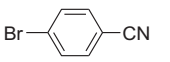	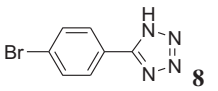 **8**	3.0	95
9	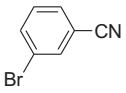	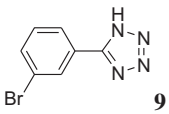 **9**	2.5	90
10	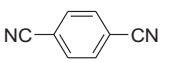	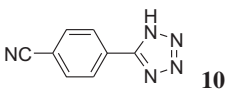 **10**	1.5	85
11	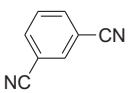	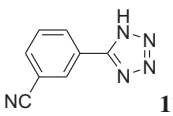 **11**	2.0	80
12	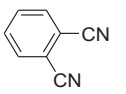	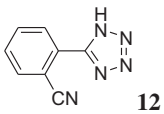 **12**	3.5	80
13	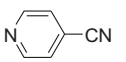	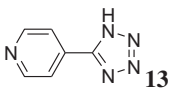 **13**	3.0	85
14	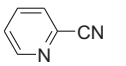	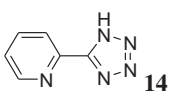 **14**	4.0	85

[a] Isolated yield.

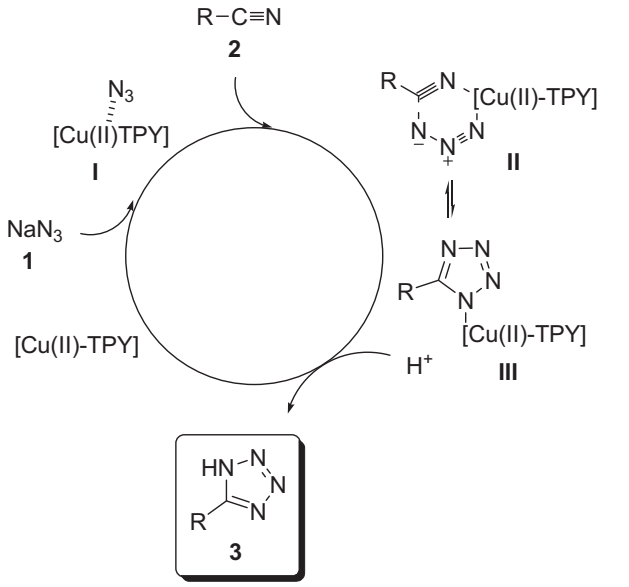

Scheme 4. A plausible mechanism for the formation of 5-substituted 1*H*-tetrazol.

presence of 4.0 mol-% of heterogeneous catalyst in the first run. The heterogeneous catalyst, which recovered by filtration after each reaction, can be reused for 5 successive times in the new experiments without dramatic yield loss and generate products with purities similar to those obtained in the first run (Fig. 4), which shows that there is no considerable change in the catalytic activity of the catalysts even after five reaction cycles.

3.4. Synthesis of 1-substituted-1H-tetrazoles

Spurred with the success of 5-substituted 1*H*-tetrazol synthesis, the formation of 1-substituted-1*H*-tetrazoles was studied using this efficient nanocatalyst. Some modifications of the previously optimized experimental protocol (Scheme 5) were required to verify that, in the presence of copper nano-catalyst (4 mol%), amine, NaN_3 and $CH(OEt)_3$ in a 1:1.3:1 M ratio are smoothly converted to 1-substituted-1*H*-tetrazoles in satisfactory yield (Scheme 5). Here the appropriate solvent was water. As previously demonstrated, the heterogeneous catalyst is recyclable and its activity is retained after five reaction cycles.

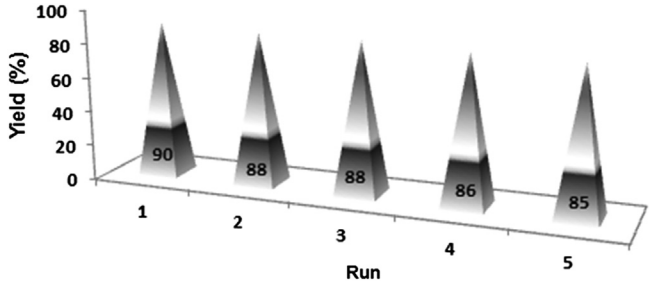

Fig. 4. Reusability of catalyst.

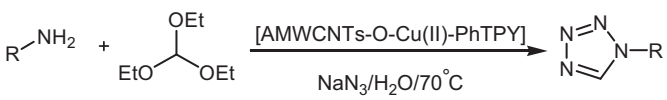

Scheme 5. One-pot synthesis of 1-substituted 1*H*-tetrazol with copper nano-catalyst.

Table 3
Synthesis of 1-substituted-1*H*-1,2,3,4-tetrazoles from various amines (1.0 mmol), triethyl orthoformate (1.0 mmol) and sodium azide (1.3 mmol) in the presence of [AMWCNTs-O–Cu(II)–PhTPY] (4.0 mol%).

Entry	Amine	Product	Time [h]	Yield [%][a]
1	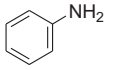	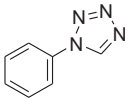 **15**	1.0	95
2	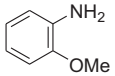	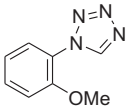 **16**	1.2	89
3	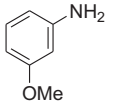	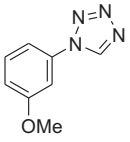 **17**	1.0	94
4	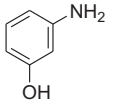	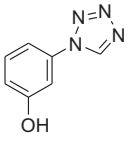 **18**	1.0	95
5	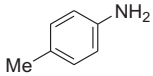	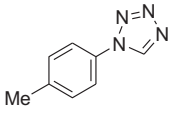 **19**	0.8	95
6	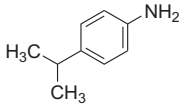	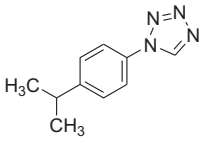 **20**	1.0	90
7	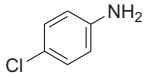	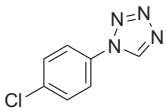 **21**	2.0	90
8	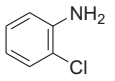	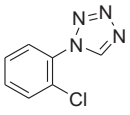 **22**	2.0	90
9	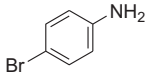	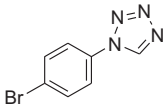 **23**	2.5	88
10	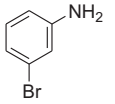	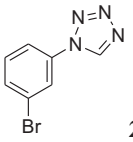 **24**	3.0	90
11	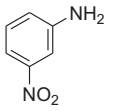	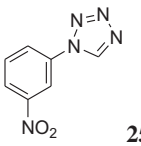 **25**	4.0	80

(*continued on next page*)

Table 3 (*continued*)

Entry	Amine	Product	Time [h]	Yield [%][a]
12	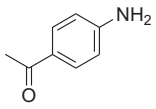	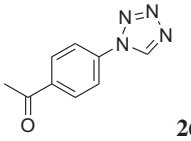 **26**	2.5	92

[a] Isolated yield.

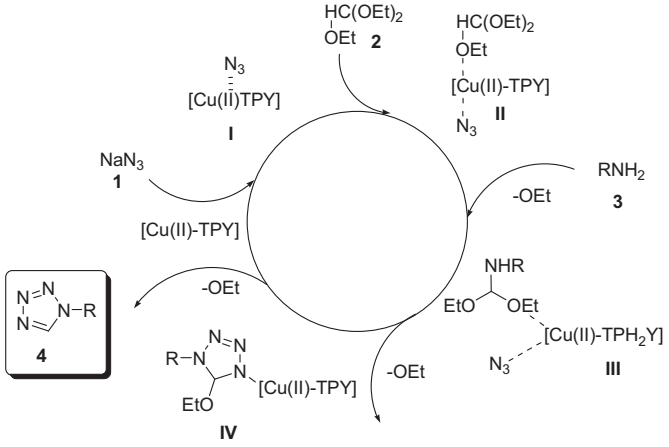

Scheme 6. A plausible mechanism for the formation of 1-substituted 1*H*-tetrazol.

As shown in Table 3, aniline and a series of its substituted derivatives, bearing a variety substituents (and their isomers), containing electron-withdrawing or electron-donating groups such as chloro, bromo, nitro, acetyl, alkoxy and alkyl underwent condensation in reasonable reaction times with excellent isolated yields (Table 3, Entry 2–12). However, applying nitro aniline as an electrondeficient amine was accompanied by the elongation of the reaction times to 4 h with the production of the desired product in 80% yields (Table 3, Entry 11).

A proposed mechanism for the 1-substituted tetrazole-forming reaction is shown in Scheme 6. It is clear from the sequence of steps that the role of [AMWCNTs-O–Cu(II)–PhTPY] is complexation of NaN_3 with [Cu(II)–TPY] complexes, activation of ethoxy groups and cleavage of C–O bonds. It can generate carbenium ions that are resonance stabilized by neighboring hetero atom O/N or readily facilitate sequential nucleophilic displacements by amine and cyclization with azide. This would explain the formation of intermediates (**II**)–(**IV**). [Cu(II)–TPY] nano-catalyst-assisted elimination of ethanol from (**IV**) leads to the final heterocycle **4**.

4. Conclusions

In summary, we have reported the use of robust and recyclable heterogeneous catalysts that provide efficient access to one-pot synthesis of various 5-substituted-1*H*-tetrazoles and 1-substituted-1*H*-tetrazoles. The use of these catalysts facilitates the implementation of high-throughput synthetic methodologies, while the exceptional efficacy of the TPY framework as copper scavenger guarantees negligible copper leaching. Other significant features of this method include its ease of operation, high efficiency, and reusability in the reaction process, which provides an efficient method for synthesis of different heterocyclic systems.

Acknowledgments

We gratefully acknowledge the support of this work by the Shiraz University Research Council.

Appendix A. Supplementary data

Supplementary data related to this article can be found at http://dx.doi.org/10.1016/j.jorganchem.2013.04.013.

References

[1] R.N. Bulter, in: A.R. Katrizky, C.W. Rees, E.F.V. Scriven (Eds.), Comprehensive Heterocyclic Chemistry, vol. 4, Pergamon, Oxford, UK, 1996.
[2] E.P. Ellis, G.B. West, Progress in Medicinal Chemistry, vol. 17, Biomedical Press, 1980, p. 151.
[3] S. Narender Rao, T. Ravisankar, J. Latha, K. Sudhakar Babu, Der Pharma Chem. 4 (2012) 1093–1103.
[4] T. Narasaiaha, D. Subba Raoa, S. Rasheeda, G. Madhavaa, D. Srinivasulua, P. Brahma Naidub, C. Naga Rajua, Der Pharm. Lett. 4 (2012) 854–862.
[5] M. Ahmad Malik, S.A. Al-Thabaiti, M.A. Malik, Int. J. Mol. Sci. 13 (2012) 10880–10898.
[6] R.N. Butler, Adv. Heterocycl. Chem. 21 (1977) 323.
[7] S. Bepary, B.K. Das, S.C. Bachar, J.K. Kundu, A.S. Shamsur rouf, B.K. Datta, Pak. J. Pharm. Sci. 21 (2008) 295–298.
[8] J. Li, S.Y. Chen, J.A. Tino, Bioorg. Med. Chem. Lett. 18 (6) (2008) 5. PMID 18295486.
[9] R.J. Nachman, G.M. Coast, K. Kaczmarek, H.J. Williams, J. Zabrocki, Acta Biochim. Pol. 51 (2004) 121–127.
[10] P. Camilleri, M.W. Kerr, T.W. Newton, J.R. Bowyer, J. Agric. Food Chem. 37 (1989) 196–200.
[11] R. Damavarapu, T.M. Klapötke, J. Stierstorfer, K.R. Tarantik, Propellants Explos. Pyrotech. 35 (2010) 395–406.
[12] C. Zhaoxu, X. Heming, Propellants Explos. Pyrotech. 24 (1999) 319–324.
[13] L. Miguel Teodoro Frija, A. Ismael, M. Lurdes Santos Cristiano, Molecules 15 (2010) 3757–3774.
[14] G.I. Koldobskii, Russ. J. Org. Chem. 42 (2006) 469–486.
[15] A. Palazzi, S. Stagni, S. Selva, M. Monari, J. Organomet. Chem. 669 (2003) 135.
[16] K. Gupta, C.Y. Rim, C.H. Oh, Synlett (2004) 2227.
[17] N.T. Pokhodylo, V.S. Matiychuk, M.D. Obushak, Tetrahedron 64 (2008) 1430–1434.
[18] D. Kundu, A. Majee, A. Hajra, Tetrahedron Lett. 50 (2009) 2668–2670.
[19] Y. Boland, P. Hertsens, J. Marchand-Brynaert, Y. Garcia, Synthesis (2006) 1504.
[20] T. Jin, S. Kamijo, Y. Yamamoto, Tetrahedron Lett. 45 (2004) 9435–9437.
[21] W.-K. Su, Z. Hong, W.-G. Shan, X.-X. Zhang, Eur. J. Org. Chem. (2006) 2723–2726.
[22] T.M. Potewar, S.A. Siddiqui, R.J. Lahoti, K.V. Srinivasan, Tetrahedron Lett. 48 (2007) 1721–1724.
[23] H. Sharghi, S. Ebrahimpourmoghaddam, M.M. Doroodmand, A. Purkhosrow, Asian J. Org. Chem. 1 (4) (2012) 377–388.
[24] P.D. Stevens, J. Fan, H.M.R. Gardimalla, M. Yen, Y. Gao, Org. Lett. 7 (11) (2005) 2085–2088.
[25] P. Serp, in: P. Serp, J.L. Figueiredo (Eds.), Carbon Materials for Catalysis, John Wiley & Sons, Inc., Hoboken, NJ, 2009, pp. 309–372.
[26] M. Monthioux, P. Serp, E. Flahaut, C. Laurent, A. Peigney, M. Razafinimanana, W. Bacsa, J.-M. Broto, in: B. Bhushan (Ed.), Springer Handbook of Nanotechnology, second revised and extended ed., Springer-Verlag, Heidelberg, Germany, 2007, pp. 43–112.
[27] G. Rotas, A.S.D. Sandanayaka, N. Tagmatarchis, T. Ichihashi, M. Yudasaka, S. Iijima, Osamu Ito, J. Am. Chem. Soc. 130 (2008) 4725–4731.
[28] C.N. Moorefield, S. Li, S.-H. Hwang, C.D. Shreimer, G.R. Newkome, Chem. Commun. (2006) 1091.
[29] Z. achary, P. Demko, K.B. Sharpless, J. Org. Chem. 66 (2001) 7945–7950.